ChemistrySelect

Research Article
doi.org/10.1002/slct.202301866

Chemistry Europe
European Chemical Societies Publishing

www.chemistryselect.org

Decoration, Characterization and Antimicrobial Activity Evaluation of Novel Nano-Based 1,2-Phenylenediamine Functionalized Maleic Anhydride-Allylphenyl Ether Conjugate

Gulderen Karakus*[a] and Mehmet Atas[b]

1,2-Phenylenediamine (*o*-PDA) is a well-known fluorescent dye that enables the decoration of next-generation chemotherapeutics. A novel *o*-PDA-functionalized maleic anhydride-allyl phenyl ether (poly(MA-*alt*-APE)/*o*-PDA conjugate) was successfully synthesized according to the Ringsdorf model, which is the starting point for macromolecular prodrugs. Functional polymeric-carriers were prepared by free-radical polymerization in butyl acetate with azobisisobutyronitrile (AIBN) radical-initiator at 70 °C. The conjugation was carried out at 40 °C in *N,N*-dimethylformamide (DMF) using triethylamine (Et_3N) as the conjugation catalyst. Characterization was performed by Attenuated Total Reflectance-Fourier Transform Infrared (ATR-FTIR), Nuclear Magnetic Resonance (^{1}H-NMR), UV-Vis and Fluorescence Spectroscopy. Weight average molecular weight (M_w), number average molecular weight (M_n) and polydispersity index (PDI) (M_w/M_n) were calculated using gel permeation chromatography (GPC). The surface morphology was also elucidated by Transmission Electron Microscopy (TEM). Evaluation of antimicrobial activity against two Gram-positive bacteria (*Staphylococcus aureus, Bacillus cereus*), two Gram-negative bacteria (*Escherichia coli, Pseudomonas aeruginosa*) and one yeast *Candida albicans* was performed using the broth microdilution method according to Clinical Laboratory Standards Institute (CLSI) criteria. Interestingly, *S. aureus* was found to be more sensitive to polymer-based samples and, in particular, the minimum inhibitory concentration (MIC) of the conjugate was lower than that of ciprofloxacin used as a control compound.

Introduction

The discovery and development of targeted biologically active compounds has recently attracted scientists. The synthesis of heterocyclic compounds and the generation of serial derivative molecules is a very powerful approach in the field of drug development. In particular, heterocyclic compounds with five-membered rings are of considerable importance both in chemistry and in biology.[1] Heterocycles are generally classified according to both the size of the heterocyclic ring (number of atoms) and the type and number of heteroatoms. The most commonly used heterocyclic compounds in synthesis are those with five- and six-membered rings containing two or more different types of heteroatoms such as nitrogen (N), oxygen (O), and sulfur (S) in the ring. The most commonly used simple aromatic heterocyclic compounds are pyridine, pyrrole, furan, and thiophene, each of which has a five-membered ring composed of four carbon atoms and each one nitrogen, oxygen, or sulfur atom.[2,3] In addition, the most well-known six-membered heterocyclic aromatic structures are piperidine, pyridine, pyrimidine, pyridazine, pyrazine, and triazine.[4] Organic compounds derived from heterocyclic skeletons are widely available naturally and synthetically, and also their pharmaceutical applications in medicinal chemistry are crucial to human life.

Although heterocyclic compounds are found in the structure of many pharmacologically active molecules, they also play an important role in biological activity. Ring-opening and ring-closing reactions initiated with five-membered furan molecules encompass several important methods for the construction of bioactive components.[4] For example, in this study, the five-membered furan derivative 2,5-furandione, also commonly known as maleic anhydride (MA), was used as a precursor molecule for the synthesis of the vinyl-based copolymerization of maleic anhydride-allyl phenyl ether copolymer. Reactions by charge transfer complexes (CTCs) play a very important and active role in the synthesis of polymers with the desired structure and potential.[5]

In this study, the poly(maleic anhydride-*alt*-allyl phenyl ether) copolymer was synthesized via the CTCs method.[5] The heterocyclic furan-2,5-dione ring is sequentially arranged in a regular distribution on the copolymer backbone, and this ring is formed by binding with an active molecule of *o*-PDA in terms of conjugation of drugs and proteins to the polymer conjugate materials linked by a nucleophilic ring opening reaction.[6–8] Depending on the nature of the nucleophile, binary amide/ester and carboxylic acid groups are formed as a result of the ring-opening reaction with the amine (RNH_2) or alcohol (ROH) group respectively for each anhydride moiety. The carboxyl functional

[a] Assoc. Prof. Dr. G. Karakus
Faculty of Pharmacy, Department of Pharmaceutical Basic Sciences, Sivas Cumhuriyet University, 58140, Sivas, Turkey
E-mail: gulderen@cumhuriyet.edu.tr

[b] Assoc. Prof. Dr. M. Atas
Faculty of Pharmacy, Department of Pharmaceutical Microbiology, Sivas Cumhuriyet University, 58140, Sivas, Turkey

Supporting information for this article is available on the WWW under https://doi.org/10.1002/slct.202301866

group plays an important role in pharmaceuticals. Providing a biologically active compound with carboxylic acid functionality is a parameter that positively affects the water solubility of the compound. In addition, the acidic character of carboxylic acid functions is the crucial factor for pharmacophores. As a stable and neutral functionality, amides play a crucial conformational role by providing a three-dimensional framework necessary for optimal binding of the active molecule to the target enzyme by binding acidic and amide groups to each other.[9] Amides, as stable and relatively neutral carboxylic acid derivatives, play an important role in providing a three-dimensional scaffold necessary for optimal binding of the drug to the target enzyme through the linking of complex acid and amide moieties. Amide bonds [–C(=O)NH–] are an important functional group found in the backbone of organic molecules and biomolecules such as peptides, proteins, DNA and RNA. The unique feature of amide bonds is their ability to form resonant structures. Therefore, and hence they are very stable and prefer specific three-dimensional (3D) structures, which are responsible for their functionality.[10] As recently noted by Noro and co-workers, the in vivo stability of amide-linked prodrugs relies on their hydrolysis by carboxylesterases,[11] peptidases, or proteases.[12] For example, proteases are enzymes that are commonly used to hydrolyze amide bonds between two amino acids.[13]

Anhydride-containing copolymers have a wide range of uses for specific applications, notably as water solubility enhancers, starting materials for the formation of nanoparticles, surface chemical modification capabilities, synthetic macromolecular carrier system capacities, dental implants, and are effective agents in medical/diagnostic imaging.[14] Their current formulations in the field of biomedical application can be listed as polymer-based conjugates, micelles, nanoparticles, nanocapsules, nanogels, liposomes and dendrimers.

In synthetic functional polymeric materials, the interaction between polymer and active small molecule is discussed in particular in terms of polymer-drug conjugates. It was the first method proposed for the rational design of polymer-based prodrugs to develop new polyanhydride-based formulations in 1975.[15–17] This model introduced the original idea that the conjugate formed as a result of a covalent bond between the drugs or small molecules and a polymer backbone via a physiologically labile bond, which carry the drug or pharmaceutically active substances such as proteins, peptides, hormones, growth factors, enzymes, etc. are generally covalently linked to the macromolecular backbone.[18] Covalently linked polymer-drug conjugates are one of the most specialized types of drug delivery systems (DDS). They have a number of advantages over the traditional parent drug they contain, such as: fewer side effects, improved therapeutic efficacy, easier drug administration and improved patient compliance.[19] In addition, polymeric prodrugs can be produced easily and cheaply under mild reaction conditions, are easily soluble in water and show no toxic and non-immunogenic behavior.[20]

Scientists have paid more attention to polymer-drug conjugates due to the disadvantages associated with nanocapsule loading. It has previously been reported that a polymer-protein-drug conjugate is being used in clinical trials in Japan.[21,22] As reported by Tong et al. the first interesting system was developed by Duncan and Kopecek in the late 1970s as an *N*-(2-hydroxypropyl)methacrylamide (HPMA) polymer-drug conjugate as an anticancer agent, which also earned a candidate for clinical trials.[22–23] Others polymer-drug conjugates reported by Davis Laboratory (IT-101)[24,25] and Frechet et al.[26,27] were camptothecin conjugated with cyclodextrin-based polymers or dendritic polyester-drug conjugates.[28] Additionally, among the water-soluble polymer conjugates, polyethylene glycol (PEG) is widely used for drug delivery and is also approved by the Food and Drug Administration (FDA) for applications in pharmaceutical activity research.[29,30]

Phenylenediamine (PDA) molecule is a disubstituted benzene derivative that has three isomers as *o*-, *m*- and *p*-phenylenediamine. In this study, the *o*-PDA molecule was chosen as a conjugation agent for rational alternating conjugate design because of its precursor role in dye preparation and organic synthesis. It is an aromatic six-membered ring structure, also classified as an aniline derivative, which has enabled the development of various heterocyclic compounds as sulfur dispersants, fungicides, corrosion inhibitors, and pharmaceuticals.[31] For example, *o*-PDA can be used in the synthesis of various benzimidazole derivatives, which are major structural units of several biologically active drug substances and also pigments.[32] Shehta and co-workers proposed a simple laboratory strategy for the practical synthesis of some fused heterocyclic systems by cyclization of *o*-PDA with various reagents. This study also paved the way for the synthesis of other fused nitrogen-containing heterocyclic compounds with a broad spectrum of bioactivity.[33] For example, benzofused core heterocyclic compounds have many biological properties such as antitumor[34] and antirotaviral[35] activities. The reactions of *o*-PDA as a binucleophilic nitrogen system have been studied in a variety of ways to derive seven-, six-, and five-membered heterocyclic compounds.[36,37]

Polymer-mediated materials are well-established biomaterials for controlled and targeted drug delivery/uptake systems and advances in biomedical applications. Materials science specifically aims to develop multifunctional materials in a single fabric. In fact, these materials are designed as a combination of several desired properties for a specific application. As the scaffold for *o*-PDA surface conjugation, water-soluble poly[MA-*alt*-APE] copolymer was chosen for its unique polyanionic character to yield a biologically active compound. As mentioned above, PDA is an amino-disubstituted benzene molecule that has attracted attention in recent years, particularly for its potential use in a sensitive immune sensor for cancer biomarkers.

No similar study on the conjugation of poly[MA-*alt*-APE] copolymer with any chemical agent or *o*-PDA molecule was found during the literature search, hence this study is unique due to its novelty in its chemical structure. The designed conjugate was synthesized inexpensively and under very mild conditions, and has a unique chemical structure with important advantages due to the listed properties: 1) it has a mechanism involving heterocyclic structure modification, 2) it is nanomaterial-sized, 3) it has amide and carboxylic acid functionality

with regular polyanionic distribution and, 4) has the ability to dissolve in water. Given the above results of both structural characterization and antimicrobial evaluations, the p[MA-*alt*-APE/*o*-PDA] composite requires further analysis to better assess its potential biological importance (e.g. fluorescent probe capacity).

Experimental section

Materials

Maleic anhydride (MA, prior to copolymerization a further purification procedure by recrystallization from dry benzene was used), butyl acetate and propyl alcohol were supplied by Merck (Schuchardt, Germany). The fluorescent 1,2-phenylenediamine (*o*-PDA) molecule and allyl phenyl ether (APE) were provided by Merck (Darmstadt, Germany). Azobisisobutyronitrile (AIBN) was supplied by Peaxnm (Russia). Ethanol (95%) was provided by Carlo-Erba (Rodano, Italy). The reagents and chemicals used for the copolymerization, modification and purification steps were of analytical grade.

Instrument

The FTIR spectrum of poly(MA-*alt*-APE) copolymer and poly(MA-*alt*-APE)/*o*-PDA conjugate was recorded using an FTIR spectrophotometer (Bruker Mode: Tensor II) at 400–4000 cm^{-1}. Nuclear magnetic resonance, ^{1}H-NMR spectra were measured at 400 MHz (JEOL, JNM-ECZ400S/L1). NMR analyses were performed after 6 mg of the samples were taken and dissolved in 0.8 mL chloroform-D. UV-Vis (Shimadzu 3600 spectrophotometer) and fluorescence spectroscopy (Agilent Technologies Cary Eclipse Fluorescence) were also used for surface morphology of the samples and examined with Transmission Electron Microscopy (TEM) (FEI/Tecnai G2 Spirit TWIN/BioTWIN CTEM a 20120 kV/LaB6). The number average (M_n), weight average (M_w) molecular weights and polydispersity index (PDI) of the samples were calculated using gel permeation chromatography (GPC) as a measure of the width of the molecular weight distribution.

Synthesis of poly(MA-alt-APE) carrier

Poly(maleic anhydride-*alt*-allyl phenyl ether) [Poly(MA-*alt*-APE)] [Ratio of monomer units ratio in copolymer (m1:m2) = 1:1] was traditionally synthesized by initiating a free radical initiator (azobisisobutyronitrile, AIBN (0.1%)) *via* charge transfer complex polymerization (CTC), 50/50 in butyl acetate, at 70 °C under a nitrogen atmosphere (Scheme 1) (Table 1).[38] The monomers MA and APE were reacted by dissolving 4.9 g of the monomer MA in 10 mL of butyl acetate in a 100 mL flask in a molar ratio of about 1:1 and then adding 4.63 mL of APE. The total volume was made up to 25 mL by adding 15 mL of butyl acetate, and a homogeneous mixture was obtained with constant shaking at room temperature. The reaction mixture was continuously purged with nitrogen gas and the polymerization reaction was terminated after 1 hour and cooled to room temperature. The product was purified by precipitation in propyl alcohol and washed several times with propyl alcohol to remove residual monomers and dried at room temperature after filtering through analytical filter paper using a vacuum filtration system.[5] The precipitate, poly(MA-*alt*-APE), was purified by drying in a vacuum oven at 55 °C for 24 h to remove the solvents used in the synthesis and precipitation.[39]

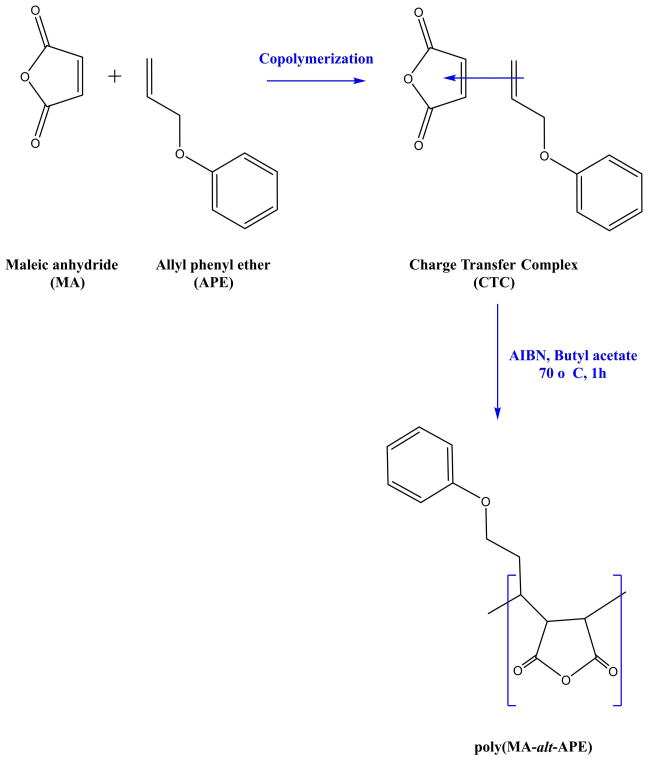

Scheme 1. Polymerization reaction of the poly(MA-*alt*-APE) copolymer.[5]

Table 1. Reaction conditions for the poly(MA-*alt*-APE) copolymer and the poly(MA-*alt*-APE)/*o*-PDA conjugate.

Sample	Molecular proportions	Initiator/catalyst	Solvents	Time (h)
p(MA-*alt*-APE)	MA:APE 1:1	AIBN[a]	Butyl acetate	1
p(MA-*alt*-APE)/*o*-PDA	Poly(MA-*alt*-APE):*o*-PDA 1:1	Et_3N[b]	DMF[c]	6

[a] AIBN: azobisisobutyronitrile. [b] Et_3N: triethylamine. [c] DMF: *N,N*-dimethylformamide

o-PDA surface functionalization of poly(MA-*alt*-APE) carrier

By modifying poly(MA-*alt*-APE) copolymer with fluorescent *o*-PDA dye molecule at a 1:1 molar ratio, in dimethylformamide (DMF) and utilizing triethylamine (Et_3N) as a conjugation catalyst for 6 h at 40 °C (Scheme 2), a poly(MA-*alt*-APE) copolymer-based conjugate was created (Table 1).[7] In order to obtain a homogenous solution, the poly(MA-*alt*-APE) copolymer powder (0.5 mmol, 116.12 mg) was thoroughly dissolved in 3 mL of well-stirred DMF. The well-mixed poly(MA-*alt*-APE)-DMF solution was then gently added to the Et_3N (15 μL). The fluorescent dye molecule *o*-PDA (0.5 mmol, 54.07 mg) was dissolved in DMF (2 mL) and then added carefully into the previous solution of poly(MA-*alt*-APE) at room temperature.[7] The final mixture was collected in a 250 mL two-necked Radleys flask with a reflux condenser, and the viscous solution was produced after 6 hours of stirring by shaking in the dark at 40 °C. The resultant precipitate was then separated from the viscous solution by centrifugation for five minutes at a speed of 6000 rpm. The viscous solution was then repeatedly rinsed with excess cold diethyl ether. The poly(MA-*alt*-APE)/*o*-PDA precipitate was ground into a

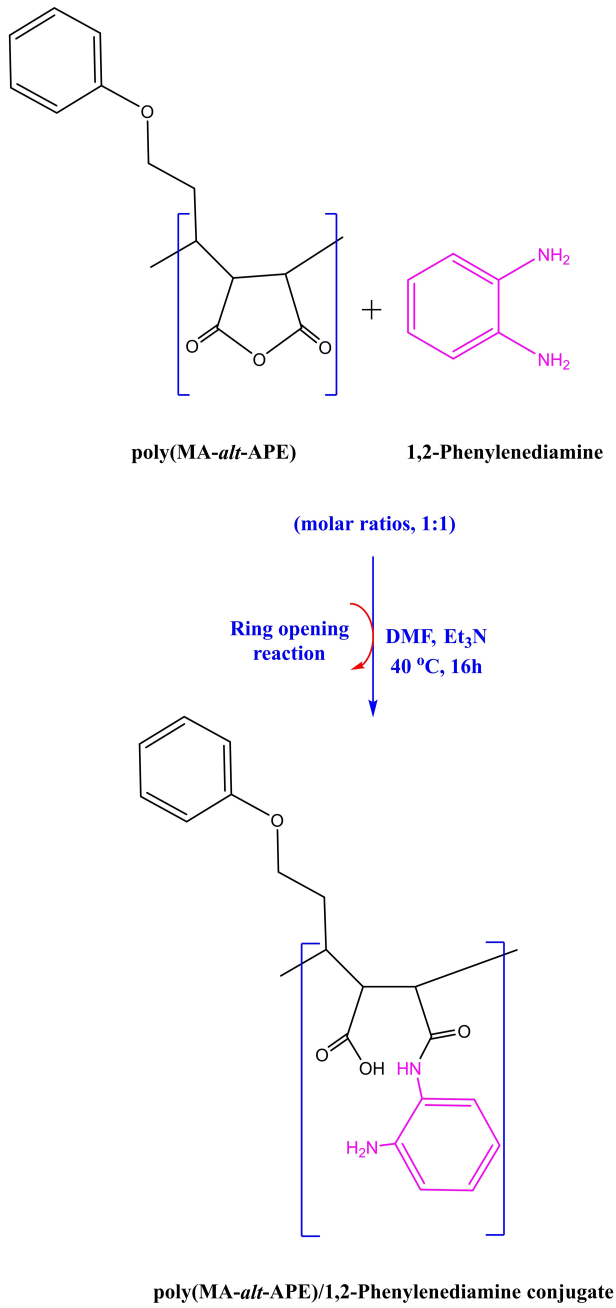

Scheme 2. Schematic representations of the *o*-PDA surface functionalization reaction of the poly(MA-*alt*-APE) copolymer.

powder and dried for 24 h at 50 °C in a vacuum incubator to produce a pure conjugate form.

Characterization

Attenuated total reflectance-fourier transform infrared spectroscopy (ATR-FTIR) measurement

ATR-FTIR spectra of the samples were recorded with a Bruker Mode: Tensor II spectrophotometer in the range of 400 to 4000 cm^{-1} in 4 cm^{-1} increments.

Nuclear magnetic resonance (^{1}H-NMR) analysis

^{1}H-NMR spectra were measured at 400 MHz (JEOL, JNM-ECZ400S/L1). Samples were prepared by dissolving 6 mg of copolymer, conjugation agent, and conjugate in 0.8 mL of chloroform-D.

UV-Visible spectral analysis

All samples in dried powder form were fresh, daily prepared solutions of 1 mg/mL ethyl alcohol and were monitored at wavelengths from 190 to 900 nm in 25 nm steps by scanning the maximum absorption bands with a UV-Vis spectrophotometer (Shimadzu 3600) absolute ethyl alcohol at room temperature as solvent and reference.

Fluorescence spectral analysis

All samples in dried powder form were freshly prepared daily solutions of 3 mg/10 mL dimethyl sulfoxide (DMSO) and were monitored at wavelengths from 400 to 800 nm with a fluorescence spectrophotometer (Agilent Technologies Cary Eclipse Fluorescence) at room temperature using DMSO as the solvent and reference.

Transmission electron microscopy (TEM)

Nanoscale structures of anhydride-containing copolymers and *o*-PDA-conjugated samples were studied using a high-resolution TEM called FEI/Tecnai G^2 Spirit BioTWIN equipped with a single-slope tomography holder for morphology identification. All samples were suspended in distilled water, dropped onto carbon film-coated copper grids, and dried at room temperature, and measurements were made at 120 kV.

Gel permeation chromatography (GPC)

The average molecular weight distribution of poly(MA-*alt*-APE) and poly(MA-*alt*-APE)/*o*-PDA was determined by a refractive index gel permeation chromatography (GPC) system. The ratio of M_w to M_n is also used to calculate the polydispersity index (PDI) of the polymer-based samples, which provides an indication of the molecular weight range of the materials. The analysis conditions are set as follows: VE 3580 RI detector, TGuard + 2xT6000M column, solvent: tetrahydrofuran (THF), detector temperature: 35 °C, column temperature: 35 °C, injection volume: 100 µL, flow rate: 1 mL/min and analysis time: 40 min/per sample.

General test for water solubility

The copolymer (0.1 g) and the solvent (10 mL, water was chosen as the solvent) were placed in a 10 mL airtight glass vial and shaken at about 25 °C at a constant speed for 1 hour. This experiment for the copolymer was repeated for the conjugate under the same conditions. In this experiment; observation of a single-phase, clear, gel-free solution is considered soluble in the solvent used.[40]

Antimicrobial activity

Broth microdilution method

Antimicrobial activity of p[MA-*alt*-AFE], *o*-PDA and p[MA-*alt*-AFE]/*o*-PDA against two Gram-positive bacteria (*Staphylococcus aureus* ATCC 29213, *Bacillus cereus* ATCC 11778), two Gram-negative

Bacteria (*Escherichia coli* ATCC 25922, *Pseudomonas aeruginosa* ATCC 27853) and one yeast *Candida albicans* ATCC 10231 were evaluated using the broth microdilution method according to Clinical Laboratory Standards Institute (CLSI) criteria with some modifications.[41,42] Samples were dissolved in DMSO (*o*-PDA, p[MA-*alt*-AFE] and p[MA-*alt*-AFE]/*o*-PDA as 20 mg/ml). In this study, Mueller Hinton Broth (Accumix®AM1072) and Sabouraud Dextrose Broth (Himedia ME033) were used as medium for bacteria and yeast, respectively. In the experiment performed in a 96-well microplate, 90 μL of the medium was added to the 1th column and 50 μL of the medium to the 2 th to 10th columns. 10 μL of the chemical compounds were added to column 1 and two-fold serial dilutions were made. 50 μL of bacteria and yeast were added such that the final concentration was 5×10^5 CFU/mL for bacteria and $0.5–2.5\times10^3$ CFU / mL for yeast in each well. Only 100 μL of medium were added to the 11th column for sterilization control. 50 μL of microorganism and 50 μL of broth were added to the 12th column as a reproduction control. The concentration of chemical compounds in the wells ranged from 1 to 0.00195 mg/mL (*o*-PDA, p[MA-*alt*-AFE] and p[MA-*alt*-AFE]/*o*-PDA). The microplates were incubated at 35 °C for 48 h for *Candida albicans* ATCC 10231 and at 37 °C for 24 h for the bacteria. After incubation, the lowest concentration that inhibits the growth of bacteria and yeast was accepted as the minimum inhibitory concentration (MIC) value.[41,42]

Results and discussion

Attenuated total reflectance-fourier transform infrared spectroscopy (ATR-FTIR) measurement

According to the information data literature review, the infrared absorption bands of *o*-phenylenediamine have the peak assignments (*s*: sharp, *m*: medium, *w*: weak, *b*: broad, and *sh*: shoulder) depicted in Figure 1a. bending deformation of the -NH fragment in primary aromatic amines at 461 cm^{-1} (*m*), bending deformation out of the plane of the -CH moiety in the 1,2-disubstituted benzene ring at 743 cm^{-1} (*b*), deformation out of plane in the benzene ring associated with the disubstitution at 804 cm^{-1} (*s*), characteristic plane -CH deformation of 1,2-disubstitution of the benzene ring at 1057 cm^{-1} (*m*) and 1116 cm^{-1} (*s*), symmetric stretching vibration for the aromatic C–C ring at 1498 cm^{-1} (*s*) and stretching of the C–N or combination band stretching for protonated primary aromatic amine at 1590 cm^{-1} (*s*), –NH deformation of secondary amine at 1628 cm^{-1} (*s*), symmetrical N–H stretch at 3027 cm^{-1} (*sh*) and symmetric =CH stretch at 3363 cm^{-1} (*s*).[43,44]

The copolymer (Figure 1b) had the anhydride ring at 1847 and 1776 cm^{-1}, which are expected to belong to the symmetric and asymmetric carbonyl stretches (–C=O) of maleic anhydride (MA), respectively.[45,46] Strong, broad CO–O–CO skeletal vibrations of the anhydride ring were recorded at 1031 and 929 cm^{-1}.[47] The characteristic C–C ring stretching was observed at 1597 cm^{-1} and 603 cm^{-1}, and C–H stretching was also observed at 2939 cm^{-1}.[48–50] In the spectrum, the peaks appear at 690 and 751 cm^{-1} in the aromatic region can be assigned to the out-of-plane =CH bend of the monosubstituted benzene moiety.[51,52] In addition, characteristic C–H (aromatic ring) bands were observed at 3362 and 3384 cm^{-1}.[6] The peak at about 1230 cm^{-1} of the spectrum is believed to belong to the stretching vibration of the C–O and C–C groups.[53] Finally, considering the main chemical structure of the poly(MA-*alt*-APE) copolymer given in Scheme 1, it was concluded that all peak assignments observed in the spectrum were compatible with this structure.

According to the structures of the poly(MA-*alt*-APE) copolymer and the poly(MA-*alt*-APE)/*o*-PDA conjugate shown in Scheme 2, aromatic peaks originate from both monosubstituted benzene rings in the spectrum found the copolymer backbone and the disubstituted benzene ring in *o*-PDA (Figure 1c). The peaks appearing at 690 and 750 cm^{-1} in the aromatic region are attributed to out-of-plane =CH bending of the monosubstituted benzene ring.[51,52] Bending deformation of the -NH group of the primary aromatic amine detected at 468 cm^{-1} (*m*). The symmetric stretch for the aromatic C–C ring occurred at 1495 cm^{-1} (*s*) and the C–N stretch (or combination band for protonated primary aromatic amine) was found at 1597 cm^{-1} (*s*) and 1586 cm^{-1} (*s*).[43,44] On the left side of the spectrum, some characteristic low peak intensity peaks related to the N–H

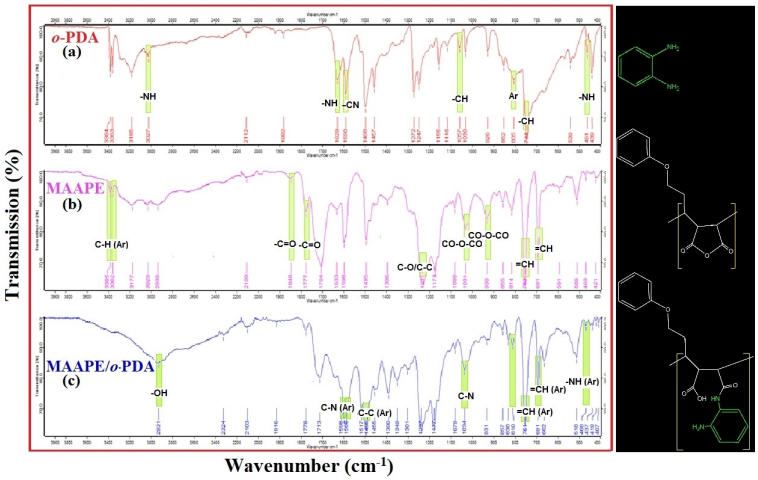

Figure 1. FTIR spectra of the copolymer, *o*-PDA, and *o*-PDA modified copolymer: (a) poly(MA-*alt*-APE), (b) *o*-PDA, and (c) poly(MA-*alt*-APE)/*o*-PDA.

stretching vibration of the *o*-PDA molecule in the region of 3300–3400 cm^{-1} were observed, but the peaks could not be identified will definitely. Stretches in the range of 690–930 cm^{-1} are characteristic substitutions on the aromatic ring. In addition, another important vibration of the disubstituted ring can be assigned to the sharp peak at 809 cm^{-1}.[54,55] Characteristic symmetric and asymmetric absorption bands of the anhydride stretches of the copolymer backbone observed at 1859 cm^{-1} for C–O-C and 1783 cm^{-1} for C=O, were completely converted to –C–N– due to the formation of amides and free acid[56,57] giving to the –C–N stretch at 1033 cm^{-1}[58,59] and the –NH vibration band at 809 cm^{-1}.[48] These frequencies were generated by a -NH bend and a –CN stretch (C–N–H),[60] indicating the monosubstituted amide bond –CONHR (Figure 1c).

The remaining peaks were assigned as follows: a C–C at 1236 cm^{-1},[53] strong O–H stretching of the carboxylic acid (–COOH) at 2930 cm^{-1} (*b*), as in the O–H bending range of 3300–2500 cm^{-1} expected of the carboxylic acid at 1390 cm^{-1} (*m*) and –C–N stretch of the aromatic amine at 1348 (*s*). Therefore, given the data obtained from the peaks observed in the spectrum, it is believed that all peak assignments are related to the poly(MA-*alt*-APE)/*o*-PDA conjugate and that the conjugate was successfully synthesized.

Nuclear Magnetic Resonance (^{1}H-NMR) Analysis

As expected, the characteristic aromatic ring protons on *o*-PDA formed a sharp peak at 6.75 and 7.2 ppm (Figure 2).[7,61–63] Hydrogen from CH groups on the aromatic phenyl ring is observed as a broad peak at ~3 ppm.

Chemical shifts for the copolymer backbone assigned to related signals as follows: monosubstituted aromatic benzene ring peaks detected at 7.02 ppm (in low intensity) and 6.48 ppm for the 2,4,6-position, at 7.25 ppm for the 3- and 5-positions, broad overlapping peaks between 1.2-1.35 ppm and 2.1, 2.6 and 2.9 ppm are due to methylene/methine protons of the ally phenyl ether and the anhydride ring.[7,64] Methine protons of the anhydride ring also appeared as a multiplet between 3.6 and 3.8 ppm.[64] The ^{1}H-NMR results confirmed the assignment of the FTIR peaks for the poly[MA-*alt*-APE)] copolymer (Figure 3).

According to the conjugation component shown in Scheme 2 in the structure of the poly[MA-*alt*-APE)]/*o*-PDA conjugate (Figure 4), in addition to the functional group peaks, both the copolymer backbone and the conjugating agent, amide and carboxylic acid functionality, formed after conjugation are also expected. The characteristic anhydride peak of poly[MA-*alt*-APE)] observed at 2.2 and 2.8–2.9 ppm is assigned to the –CH protons of the anhydride of the MA unit.[65] As a methylene bridge, CH_2 peaks of the APE unit were observed in the range of 1–2 ppm.[66,67] The characteristic aromatic ring protons on both APE (monosubstituted) and *o*-PDA (disubstituted) overlapped at 7.2 ppm and formed a sharp signal.[7,64] Confirmation of the mechanism of the conjugation reaction for poly[MA-*alt*-APE)]/*o*-PDA was performed by detecting the expected peak in the 5.0–8.5 ppm range due to the amide –NH (–CONH–) in addition to other peak assignments. Group of low-intensity protons at 8 ppm in the spectrum.[6] No significant integrated carboxylic acid peak could be observed due to the possibility of intramolecular hydrogen bonding with –NH (amide) and –OH (carboxylic acid). Considering all the peak assignments, it can be said that the presence of characteristic copolymer/conjugating agent/amide bond peaks for poly[MA-*alt*-APE)]/*o*-PDA occurred in the ring-opening reaction and the conjugation was also successful.[68]

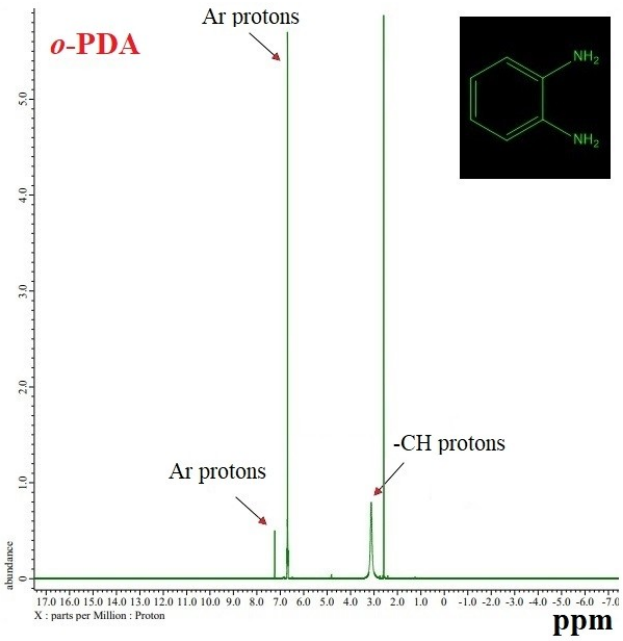

Figure 2. ^{1}H-NMR spectrum of *o*-PDA.

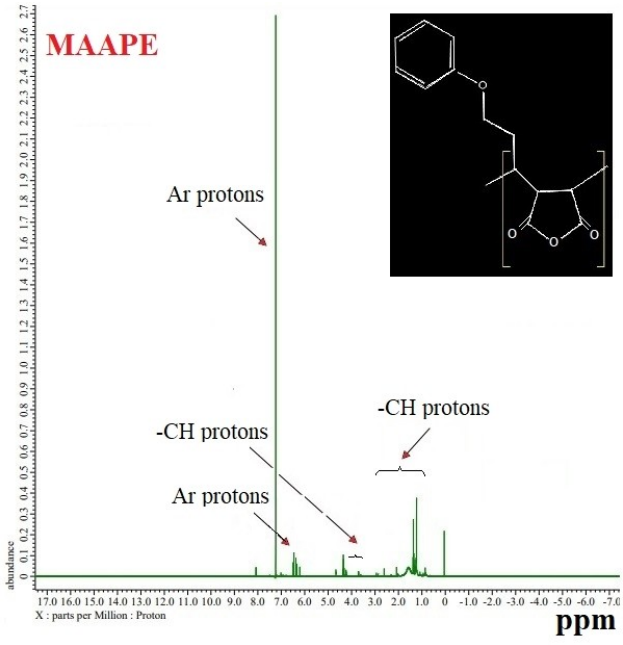

Figure 3. ^{1}H-NMR spectrum of poly(MA-*alt*-APE) copolymer.

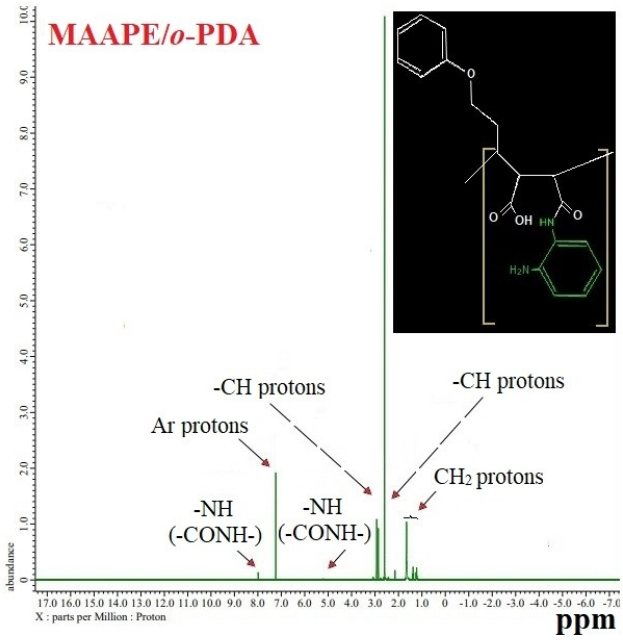

Figure 4. ^{1}H-NMR spectrum of poly(MA-*alt*-APE) /*o*-PDA conjugate.

UV-Visible spectral analysis

A comparison of the absorption spectra of poly(MA-*alt*-APE)/*o*-PDA with two similar materials, poly(MA-*alt*-APE) and *o*-PDA (Figure 5), shows that they have specific corresponding wavelengths of visible light have absorbing chemical structure for their absorption. Measurements in ethyl alcohol showed that poly(MA-*alt*-APE) and poly(MA-*alt*-APE)/*o*-PDA had a peak maximum at about max = 210 and 270 nm, while *o*-PDA appeared at λ_{max} = 294, 240, and 210 nm.

The UV-Vis spectra of *o*-PDA (Figure 5, red color) with two absorption bands appear at λ_{max} = 210 nm and 240 nm, which can be detected at the π–π transition of the disubstituted benzene ring and another absorption band at ~294 nm due of the benzene ring transition.[43] In summary, the absorption behavior of poly(MA-*alt*-APE) (Figure 5 blue color) and poly(MA-*alt*-APE)/*o*-PDA (Figure 5, green color) is in shape and very similar in intensity.

The peak of the carbonyl groups (C=O) originating from the anhydride ring in the main chain of the copolymer in the conjugate was observed at λ_{max} = 270 nm (weak n-π transition of C=O) in the spectrum of both the copolymer and the conjugate.[69] On the other hand, since the conjugation agent in *o*-PDA has no carbonyl group (C=O), no absorption peak was observed in the spectrum. The band with a longer wavelength and weaker intensity belongs to the n→π* transition of nonbonding electrons of the carbonyl group (for –COOH or –$CONH_2$) located on the oxygen atom.

Ultraviolet-Vis spectroscopy (UV-Vis) is one of the important tools for the structural characterization of polymer-based materials to confirm their chemical structure and elucidate their properties for their physical behavior.[70] It can be said that the conjugation was successful because both the carbonyl group absorption band, which is believed to belong to the anhydride, carboxyl, and amide groups, and the absorption bands of the conjugating agent and the aromatic ring in the carrier in the designed conjugate were observed.

Fluorescence spectral analysis

Scanning the absorption spectrum to record the emission intensity of the fluorescent chemical compound at a single wavelength with maximum emission intensity produces the

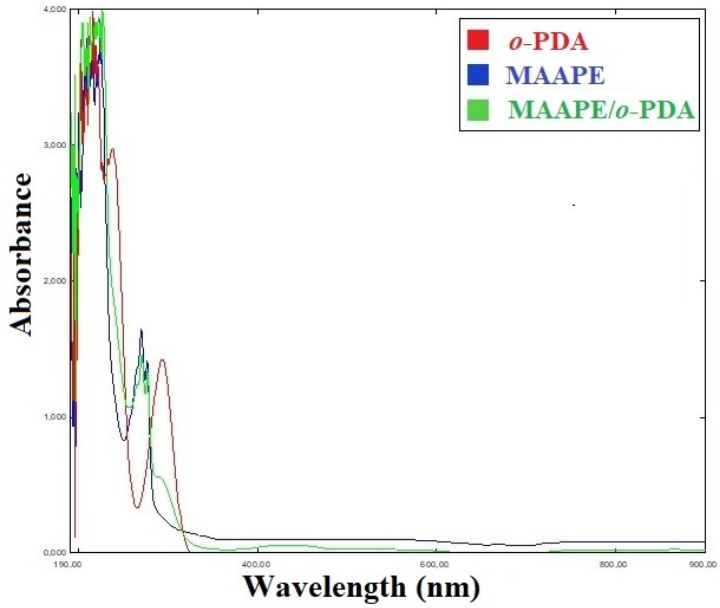

Figure 5. UV- visible spectra for poly(MA-*alt*-APE) copolymer, *o*-PDA, and poly(MA-*alt*-APE)/*o*-PDA conjugate.

excitation spectrum. That is, excitation of the compound at a single maximum absorption wavelength while scanning the emission wavelengths illuminates the emission spectral profile.

The measurement of the fluorescence emission spectrum of the copolymer, the conjugation agent and the conjugate (in DMSO, $c = 3.0\times10^{-1}$ g·L^{-1}) (Figure 6) was recorded in the wavelength range 400–800 nm. According to the results obtained by scanning the spectrum in the UV-visible region; 210, 240, about 270 and about 294 nm were chosen as the excitation wavelengths since these were peaks in the spectral scan. Since the excitation wavelength corresponds to the highest absorbance of the fluorescence measurement, no significant peak was observed for the maximum emission wavelength of *o*-PDA, but only a small shoulder at 471 nm. On the other hand, it was observed that the maximum emission wavelength of poly(MA-*alt*-APE) and poly(MA-*alt*-APE)/*o*-PDA was 585 nm and 587 nm, respectively, with a small shift.

It was observed that the spectral emission behavior of poly(MA-*alt*-APE) (Figure 6, blue color) and poly(MA-*alt*-APE)/*o*-PDA (Figure 6, red color) was quite different in shape and intensity. The decrease in intensity for the poly(MA-*alt*-APE)/*o*-PDA conjugate and the blue shift in the emission wavelength indicates that the conjugation of the poly(MA-*alt*-APE) copolymer with the *o*-PDA is novel molecule formation was successful. The sharpness of the emission peak for poly(MA-*alt*-APE) and poly(MA-*alt*-APE)/*o*-PDA indicates that the molecular weight of the molecule is increasing and the desired structure is being formed. In summary, the *o*-PDA molecule acquires a fluorescence-active property by being conjugated to the poly(MA-*alt*-APE) backbone.

It is known that the bathochromic effect (spectral shift to longer wavelengths or red shift) is observed by increasing the number of acidic groups (–COOH) increasing the fluorescence intensity.[71] On the contrary, the interaction of aromatic compounds with the target molecule leads to a drastic decrease in the fluorescence intensity.[72] On the other hand, in the excited state, polar solvents such as DMSO activate the probable intermolecular charge transfer from one part (donor) of the molecule to the other (acceptor). In addition, the conjugated form contains two N–H moieties that serve as H-bond donors and the copolymer form contains two carbonyl groups that serve as H-bond acceptors. Considering all the factors affecting the fluorescence intensity, it can be said that after conjugation, the five-membered ring of the starting molecule was opened and the carbonyl groups (–C=O) were replaced by carboxyl functional groups (–COOH) and amide bonds [–C(=O)NH–]. Although the decrease in intensity and the blue shift in emission wavelength for the poly(MA-*alt*-APE)/*o*-PDA conjugate (Scheme 2) are due to different causes, it is believed that the main reason is the increase in the number of aromatic rings.

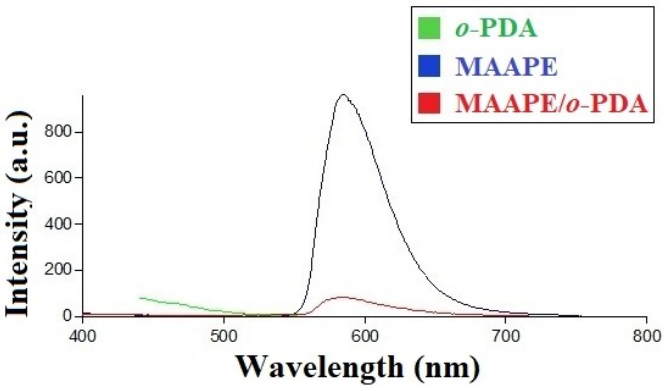

Figure 6. Fluorescence emission spectra for poly(MA-*alt*-APE) copolymer, *o*-PDA, and poly(MA-*alt*-APE)/*o*-PDA conjugate.

Transmission electron microscopy (TEM)

A nanocomposite consists of distinct phases with multiple dimensions less than 100 nm or repeating spaced nanoscale structures between the phases of the material. The nanoscale structures and surface properties of the anhydride-containing copolymer and its *o*-PDA conjugate were compared using transmission electron microscopy considering the size scale in Figure 7 (Figure 7a–b, Figure 7c–d, and Figure 7e–f) to identify the morphology. In the TEM images, samples were taken at different magnifications such as 100, 50, 200 and 500 nm. For comparison, the size scale of the conjugate was studied to be about five times larger than that of the copolymer.

Samples show nanomaterial properties with a length of 100–300 nm, with the size of the copolymer being about 117 nm (Figure 7e), while the size of the conjugate was around 230 and 280 nm (Figure 7f) at 50 or 200 nm magnification. Conjugates show good dispersion and also form nanocomposite products showing a homogeneous and compatible distribution of the *o*-PDA molecule in MA including the copolymer matrix.[73,74] It was found that the size of the conjugate was larger than that due to the size of the copolymer stronger interaction between the copolymer and the conjugate due to the good *o*-PDA compatibility (Figure 7e–f). The final product becomes more uniformly spherical and grows compared to the unmodified form because the surface of the copolymer has been changed from a partially hydrophobic to a hydrophilic character, which is consistent and more prominent with the increasing water-solubility behavior in the conjugation process.[73] It is clear that the *o*-PDA molecule is covalently bonded directly to the copolymer surface. Conjugation is also directly affected by the morphological parameters of the initial copolymer matrix.[74] The structure of the conjugate was observed to be similar to that of the copolymer and the spherical (*o*-PDA drug-loaded surface) shaped nanostructure was well compatible with the dimensions of the nanomaterial, and some non-spherical, irregular shapes were also observed at a low rate.[73]

Given spectroscopic measurement results; although the conjugate is observed to be mostly surrounded by the main chain of the copolymer, it can be said that the conjugation with the amide bond occurs through the ring opening reaction as a result of the modification of the anhydride ring on the copolymer surface with amine groups of the *o*-PDA.

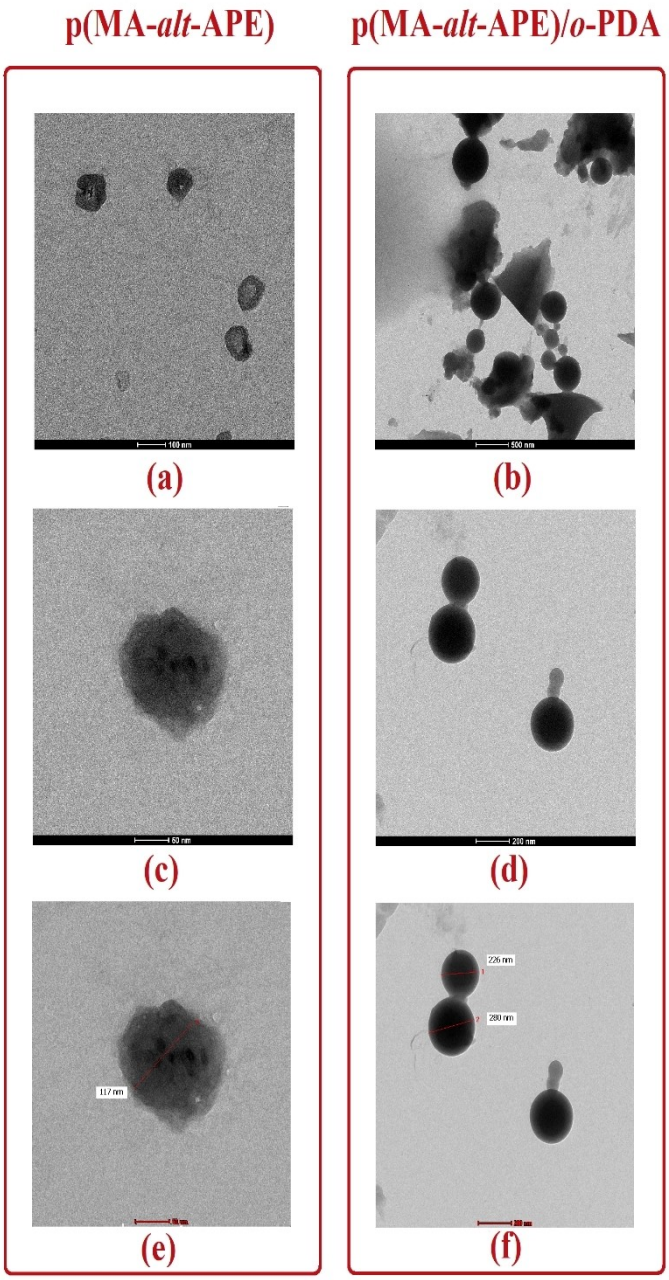

Figure 7. TEM images of for poly(MA-*alt*-APE) copolymer and poly(MA-*alt*-APE)/*o*-PDA conjugate.

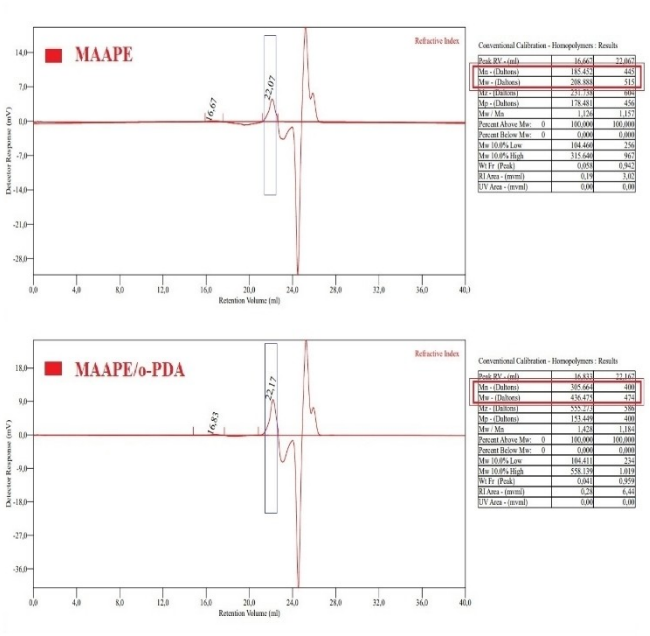

Figure 8. Gel permeation chromatogram (GPC) of poly(MA-*alt*-APE) copolymer and poly(MA-*alt*-APE)/*o*-PDA conjugate.

Table 2. Molecular weights (MW) and PDI values of Poly(MA-*alt*-APE) copolymer and the poly(MA-*alt*-APE)/*o*-PDA conjugate.

Sample	M_w[a] (10^4, Da)	M_n[b] (10^4, Da)	PDI[c] (M_w/M_n)
p(MA-*alt*-APE)	20.889	18.545	1.126
p(MA-*alt*-APE)/*o*-PDA	43.648	30.566	1.428

[a] M_w : Weight-average MW. [b] M_n : Number average MW. [c] Da: Dalton. PDI: Polydispersity index.

Gel permeation chromatography (GPC)

The molecular weight distribution of the poly(MA-*alt*-APE) copolymer and the poly(MA-*alt*-APE)/*o*-PDA conjugate (10%), the number average molecular weight (M_n) and the weight average molecular weight (M_w) were measured (Da) (Figure 8) and the polydispersity index (PDI) as a result of the M_w/M_n ratio were calculated using a refractive index gel permeation chromatography (GPC) system. M_w and PDI of the samples were summarized in Table 2 as follows: MAAPE: 20.889×104 Da (PDI = 1126) and MAAPE/*o*-PDA: 43.648×104 Da (PDI = 1428).[6,8,40]

Polydispersity arises due to size distribution or agglomeration/aggregation in a sample. The PDI is a size-based measure of the heterogeneity of a sample that the higher the PDI, the broader the molecular weight distribution.[75] While the PDI value of the synthesized copolymer was about 1.13 in this study, it increased significantly to about 1.43 for the conjugate due to the *o*-PDA modification.[76] According to the literature review, the best controlled synthetic polymers have a PDI of 1.02–1.10 and chain growth polymerization gives PDI values in the range of 1.520.[76] International standardization organizations (ISOs) have stated that a PDI value of less than 0.05 is more common for monodisperse samples, while a value above 0.7 is appropriate for a broad (e.g. polydisperse) particle distribution (ISO ISO 22.412:2017 and ISO 22.412: 2017 standards).[75] As a result, the conjugate (~1.43 compatible with the PDI value corresponding to chain growth polymerization) grows due to the increase in molecular weight of the molecule compared to the pre-modification (~1.13 compatible with the PDI value of most controlled synthetic polymers) and at the same time, after *o*-PDA surface modification, it was observed that the heterogeneity based on size increased. Since the data obtained by GPC chromatographic analysis supported the

results of spectroscopy (FTIR, ^{1}H-NMR, UV-Vis and fluorescence analysis) and morphology analysis (TEM), it was concluded that the surface modification of the copolymer with the *o*-PDA molecule was successfully achieved.

General Test for Water Solubility

The water solubility test was performed according to the general solubility test. Briefly, the copolymer (or conjugate) was dissolved in water at 25 °C for 1 hour. In this experiment; observation of a single-phase, clear, gel-free solution is assumed to be soluble in the solvent used.[40] The conjugate was considered water soluble because a single phase, clear, gel-free solution was observed, and on the other hand, the copolymer was considered partially water soluble because of the cloudy appearance in solution.[40]

Proposed reaction mechanisms for carrier and *o*-PDA functionalized conjugate

Copolymerization reaction of maleic anhydride and allyl phenyl ether depicted in Scheme 1. The reaction of acid anhydrides with amines (Scheme 2) to form the corresponding amides is represented by a four-step mechanism (Scheme 3):[6,77] 1) nucleophilic attack of the anhydride group by the aromatic amine molecule, 2) ring-opening reaction, 3) deprotonation by aromatic amine after nucleophilic attack, and 4) proton transfer/intramolecular assembly, each as per spectroscopic measurement and water-solubility test results for the structural characterization of the designed alternating copolymer and the fluorescent dye-functionalized conjugate. The ring-opening reaction occurred after nucleophilic acylation of a symmetrical carboxylic acid anhydride group, which undergoes a nucleophilic acyl substitution reaction, resulting in an amide (neutral carboxylic acid derivative).

The results of the spectroscopic analysis and the water solubility of the poly(MA-*alt*-APE)/*o*-PDA conjugate confirmed that the conjugation proceeded successfully after the ring-opening reaction via the amide mechanism.

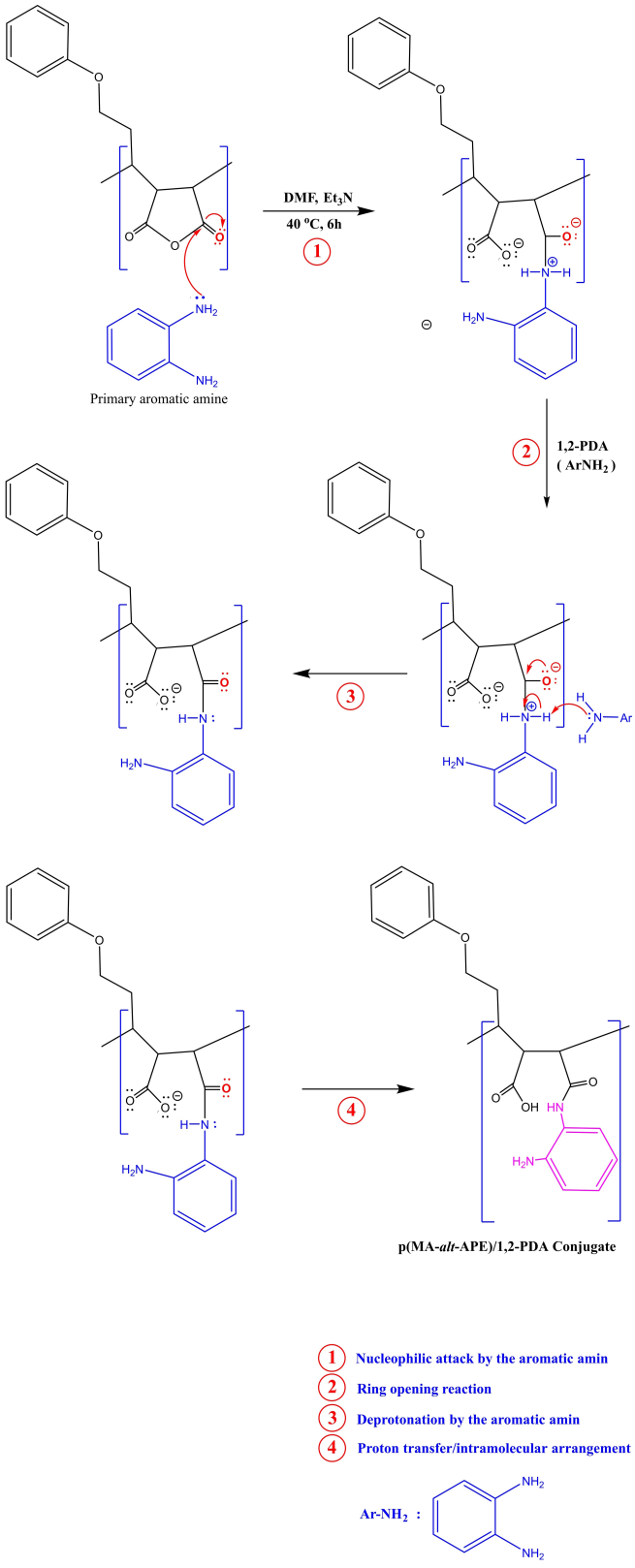

Scheme 3. Schematic representations of the *o*-PDA surface functionalized-poly(MA-*alt*-APE) reaction mechanism.

Antimicrobial activity

Broth microdilution method

Antimicrobial activity of p[MA-*alt*-AFE], *o*-PDA, and p[MA-*alt*-AFE]/*o*-PDA against two gram-positive bacteria (*Staphylococcus aureus* ATCC 29213, *Bacillus cereus* ATCC 11778), two gram-negative bacteria (*Escherichia coli* ATCC 25922, *Pseudomonas aeruginosa* ATCC 27853) and one yeast *Candida albicans* ATCC 10231 were evaluated using the broth microdilution method according to Clinical Laboratory Standards Institute (CLSI) criteria with some modifications.[41,42] Antimicrobial activities against four bacteria and *C. albicans* from poly(MA-*alt*-APE), poly(MA-*alt*-APE)/*o*-PDA, and *o*-PDA were observed in the concentration range of 0.001–1 mg/mL, the minimum inhibitory concentration (MIC) of the samples is also summarized in

Table 3. MIC[a] values of synthesized compounds on microorganisms (mg/mL).

Sample	*E.coli.* ATCC25922	*S.aureus* ATCC29213	*P.aeruginosa* ATCC27853	*B.cereus* ATCC11778	*C.albicans* ATCC10231
o-PDA	0.25	1	>1	>1	1
p(MA-*alt*-APE)	>1	0.003	>1	1	1
p(MA-alt-APE)/*o*-PDA	>1	0.001	>1	1	1
Ciprofloxacin	0.0156	0.25	1	0,125	–
Amphotericin B	–	–	–	–	0.25

[a] MIC: Minimum inhibition concentration.

Table 3. *o*-PDA was found to have a more potent MIC value (0.25 mg/mL) in *E. coli* than poly(MA-*alt*-APE) and poly(MA-*alt*-APE)/*o*-PDA (>1 mg/ml). Among the microorganisms tested, *S. aureus* was found to be more sensitive to poly(MA-*alt*-APE), poly(MA-*alt*-APE)/*o*-PDA than the *o*-PDA. Interestingly, the MIC value of the conjugate (0.001 mg/l) in *S. aureus* was lower than that of the copolymer (0.003 mg/l) and moreover the values obtained were also lower than those of ciprofloxacin (0.25 mg/ml) used as a control compound. It was found that *S. aureus* more sensitive to the synthesized samples than the other bacteria and *C. albicans*. However, the *o*-PDA, the poly(MA-*alt*-APE), and the poly(MA-*alt*-APE)/*o*-PDA showed relatively the same antimicrobial effect on the other microorganisms tested (1 or >1 mg/ml).

The fact that the synthesized polymer samples are specific only for *S. aureus* is due to the similarity of the amide functionality in their structures to the lactam. The amide functional group in the lactam is in the ring while the amide group is in the straight chain on the conjugate surface. Monobactams, penicillins, cephalosporins, and carbapenems are beta-lactam antibiotics that contain a beta-lactam ring (β-lactam, known as a cyclic amide). These are bactericidal antibiotics that inhibit penicillin-binding proteins (PBPs) through covalent binding and inhibit bacteria in the cytoplasmic membrane. It was concluded that the conjugate, like antimicrobials, is particularly sensitive to *S. aureus* species as its MIC value is lower than that of ciprofloxacin. This sensitivity can be explained in particular by newly formed functional groups on the surface of the polymer-based conjugate. As shown in Scheme 2, in the conjugated form there are amide bonds and carboxylic acids, which are believed to be functional groups that cause bacterial susceptibility. Furthermore, increasing the alkyl chain length and hydrophobicity of the polymer-based material increases its affinity for binding to the lipid membrane, leading to cell death after membrane rupture. Furthermore, polymers with amphiphilic and cationic groups first destroy the bacterial membrane through electrostatic interaction, killing the bacterial cell and reducing the resistance of the bacteria by invading the lipid regions of the membrane[78,79] Finally, considering the studies on antimicrobial polymers, the bactericidal mechanism of the conjugate, which contains an extended alkyl chain in addition to amide and carboxylic acid functional groups, can be explained in two ways:[80] 1) electrostatic interaction between polymer-based samples and bacterial cell wall, and 2) polymer-based structures targeting the cytoplasmic membrane.

Conclusions

According to the literature search, no similar study on the *o*-PDA surface derivatization of the maleic anhydride allyl phenyl ether copolymer has been found so far, except for the copolymer synthesis by Zengin et al.[5] This study is based on the preparation of a new copolymer and copolymer-anchored conjugate design, the characterization of these structures using current spectroscopic, morphological and chromatographic methods, and the investigation of the antimicrobial activity potential. The chemical process of the synthesized products involved the preparation of the functional and water-soluble MA-based copolymer and the nucleophilic ring opening of the anhydride units on the copolymer backbone by the fluorescent dye molecule (*o*-PDA). Spectroscopic analysis and water solubility results confirmed that derivatization was successfully achieved via the amide mechanism. In the results of TEM and GPC analysis, it was also emphasized that in the *o*-PDA substitution on the conjugated surface, the copolymer backbone grew about twice after the conjugation, and it was concluded that this growth was homogeneous, and a uniformly distributed structure was achieved.

The designed conjugate can be evaluated from two perspectives: 1) *o*-PDA is an aromatic disubstituted amino precursor molecule to produce many heterocyclic compounds and can also be easily oxidized by various oxidizing agents to produce fluorescent compounds, promoting its use as a cancer biomarker in the sensitizing immune sensor has recently attracted attention. 2) Aromatic rings are widely used as an important part of drug design in medicinal chemistry to enable fragment-based drug design (FBDD).[81] Particularly preferred the bulk structure of drugs because of their known synthetic pathways and modification mechanisms.[82] These are the main contributions of our proposed design that there are many aromatic rings arising both from the copolymer and from the conjugate's own backbone and the attached *o*-PDA molecule (Scheme 1 and 2). On the other hand, the antimicrobial activity assessment promised that *S. aureus* was more sensitive to polymer-based samples and, in particular, the minimum inhib-

itory concentration (MIC) of the conjugate was lower than that of ciprofloxacin used as a control compound.

It is believed that the synthesized conjugate can be functional and useful materials that have the potential to be used as a controlled-release nanocomposite, especially in antimicrobial treatment, and that aromatic rings also occupy a significant part of the molecule and functional drugs and prodrugs structures play a role in the synthesis. Therefore, it is hypothesized that the synthesized carrier and conjugate can structurally serve this research area and be redesigned according to the desired properties.

Supporting Information Summary

Some of the experimental details such as ATR-FTIR spectroscopy measurements and transmission electron microscopy (TEM) images have been provided in the Supporting Information.

Acknowledgements

Copolymer and conjugate syntheses and microbiological tests were carried out in the Research Laboratories of Basic Pharmaceutical Sciences and Microbiology of the Faculty of Pharmacy, Sivas Cumhuriyet University. The structural characterization analysis measurements were carried out by Sivas Cumhuriyet University Advanced Technology Research and Application Center (CUTAM), Sivas, Turkey. Transmission electron microscopy (TEM) images were acquired from the Central Laboratory of the Middle East Technical University (METU).

Conflict of Interests

There are no conflicts to declare.

Data Availability Statement

The data that support the findings of this study are available from the corresponding author upon reasonable request.

Keywords: antimicrobial activity · 1,2-phenylenediamine · poly(MA-*alt*-APE) copolymer · structural characterization · surface modification

[1] G. W. Gribble, J. A. Joule, *Five-Membered Ring Systems: With More than One N Atom. In Progress in Heterocyclic Chemistry*, Elsevier: Amsterdam, **2020**, p. 325.
[2] T. Kunied, H. Mutsanga, *The chemistry of heterocyclic compounds*, Palmer, B, **2002**, p. 175.
[3] S. Jaiswal, *Int. J. Mod. Trends. Sci. Technol.* **2019**, *5*, 36–39.
[4] J. A. Joule, Keith Mills, *Heterocycl. Chem.*, A John Wiley & Sons, Ltd., Publication, West Sussex, **2010**, p.689.
[5] H. B. Zengin, A. Boztug, S. Basan, *J. Appl. Polym. Sci.* **2006**,*101*, 2250–2254.
[6] G. Karakus, A. Ece, A. Sahin-Yaglioglu, H. B. Zengin, M. Karahan, *Polym. Bull.* **2017**, *74*, 2159–2184.
[7] G. Karakus, *Hittite J. Sci. Eng.* **2022**, *9*, 305–311.
[8] G. Karakus, Z. Akin-Polat, A. Sahin-Yaglioglu, M. Karahan, A. F. Yenidunya, *J. Biomat. Sci. Polym.* E. **2013**, *24*, 1260–1276.
[9] C. Lamberth, J. Dinges, *Different Roles of Carboxylic Functions in Pharmaceuticals and Agrochemicals.* In Bioactive Carboxylic Compound Classes. **2016**, https://doi.org/10.1002/9783527693931.ch1.
[10] S. Mahesh, K.-C. Tang, M. Raj, *Molecules* **2018**, *23*, 2615.
[11] D. Wang, L. Zou, Q. Jin, J. Hou, G. Ge, L. Yang, *Acta. Pharm. Sinic.* **2018**, *B 8*, 699–712.
[12] P. Philipps-Wiemann, Enzymes in Human and Animal Nutrition (Ch 12, Proteases-general aspects), C. S. Nunes, V. Kumar (Eds.), Academic Press, **2018**, p. 257.
[13] J. Noro, T. G. Castro, A. Cavaco-Paulo, C. Silva, *Process Biochem.* **2020**, *98*, 193–201.
[14] I. Popescu, D. M. Suflet, I. M. Pelin, G. C. Chitanu, *Rev. Roum. Chim.* **2011**, *56*, 173–88.
[15] H. Ringsdorf, *J. Polym. Sci. Part C* **1975**, *51*, 135–153.
[16] R. Duncan, *Res. Focus. Rev.* **1999**, *2*, 441–449.
[17] K. Hoste, K. D. Winne, E. Schacht, *Int. J. Pharmaceut.* **2004**, *277*, 119–131.
[18] C. Elvira, A. Gallardo, J. S. Roman, A. Cifuentes, *Molecules* **2005**, *10*, 114–125.
[19] C. Li, S. Wallace, *Adv. Drug Delivery Rev.* **2008**, *60*, 886–898.
[20] E–R. Kenawy, F. Abdel-Hay, M. El-Newehy, R. M. Ottenbrite, *Polym. Int.* **2008**, *57*, 85–91.
[21] R. Tong, J. J. Cheng, *Polym. Rev.* **2007**, *47*, 345–381.
[22] R. Duncan, *Nat. Rev. Cancer* **2006**, *6*, 688–701.
[23] R. Duncan, *Nat. Rev. Drug Discovery* **2003**, *2*, 347–360.
[24] J. Cheng, K. T. Khin, G. S. Jensen, A. Liu, M. E. Davis, *Bioconjugate Chem.* **2003**, *14*, 1007–17.
[25] M. E. Davis, *Mol. Pharm.* **2009**, *6*, 659–68.
[26] M. E. Fox, F. C. Szoka, J. M. J. Frechet, *Acc. Chem. Res.* **2009**, *42*, 1141–1151.
[27] C. C. Lee, E. R. Gillies, M. E. Fox, S. J. Guillaudeu, J. M. J. Frechet, E. E. Dy, F. C. Szoka, *Proc. Natl. Acad. Sci. USA* **2006**, *103*, 16649–54.
[28] R. Tong, L. Tang, N. P. Gabrielson, Q. Yin, J. Cheng, *Polymer–Drug Nanoconjugates, Pharmaceutical Sciences Encyclopedia: Drug Discovery, Development, and Manufacturing*, John Wiley & Sons, Inc., New York, **2013**, https://doi.org/10.1002/9780470571224.pse494.
[29] V. G. Kadaji, C. V. Betageri, *Polymer* **2011**, *3*, 1972–2009.
[30] K. Cho, X. Wang, S. Nie, Z. G. Chen, D. M. Shin, *Clin. Cancer Res.* **2008**, *14*, 1310–1316.
[31] R.-J. Yu, J.-J. Sun, H. Song, J.-Z. Tian, D.-W. Li, Y.-T. Long, *Sensors* **2017**, *17*, 530.
[32] her>https://www.sigmaaldrich.com.
[33] W. Shehta, M. G. Assy, N. A. Ismail, A. M. Almostafa, *Russ. J. Org. Chem.* **2021**, *57*, 1152–1157.
[34] M. Yoshida, I. Hayakawa, N. Hayashi, T. Agatsuma, Y. Oda, F. Tanzawa, S. Iwasaki, K. Koyama, H. Furukawa, S. Kurakatad, Y. Suganob, *Bioorg. Med. Chem. Lett.* **2005**, *15*, 3328–3332.
[35] T. R. Bailey, D. C., Pevear PCT, *PCT Int. Appl*, WO2004078115, **2004**.
[36] P. S. Rathee, R. Dhankar, S. Bhardwaj, M. Gupta, R. Kumar, *J. Appl. Pharmacol.* **2011**, *1*, 127–130.
[37] K. Padmavathy, N. Gopalpur, K. V. Geetha, *Tetrahed. Lett.* **2011**, *52*, 544–547.
[38] G. Karakus, *Marmara Pharm. J.* **2015**, *19*, 121–125.
[39] D. Spridon, L. Panaitescu, D. Ursu, C. V. Uglea, I. Popa, R. M. Ottenbrite, *Polym. Int.* **1997**, *43*, 175–181.
[40] M. H. Nasirtabrizi, Z. M. Ziaei, A. P. Jadid, L. Z. Fatin, *Int. J. Ind. Chem.* **2013**, *4*, 11.
[41] CLSI, Reference Method for Broth Dilution Antifungal Susceptibility Testing of Yeasts. Approved Standard. CLSI document M27-A3, Clinical and Laboratory Standards Institute, Wayne, PA, USA, 3rd edition, **2008**.
[42] CLSI, Methods for Dilution Antimicrobial Susceptibility Tests for Bacteria that Grow Aerobically, Approved Standard, 9th ed., CLSI document M07-A9. Clinical and Laboratory Standards Institute, 950 West Valley Road, Suite 2500, Wayne, Pennsylvania 19087, USA, **2012**.
[43] S. M. Sayyah, A. B. Khaliel, A. A. Aboud, S. M. Mohamed, *Int. J. Polym. Sci.* **2014**, *2014*, 16.
[44] J. Guay, L. H. Dao, *J. Electroanal. Chem. Interfacial Electrochem.* **1989**, *274*, 135–142.
[45] K. J. Yoon, J. H. Woo, Y. S. Seo, *Fiber. Polym.* **2003**, *4*, 182–187.
[46] C. M. Xiao, J. Tan, G. N. Xue, *eXPRESS Polym. Lett.* **2010**, *4*, 9–16.
[47] G. C. Chitanu, I. Popescu, A. Carpov, *Rev. Roum. Chim.* **2006**, *51*, 923–929.
[48] Z. M. O. Rzayev, *Int. Rev. Chem. Eng.* **2011**, *3*, 153–215.

[49] J. Pal, H. Singh, A. K. Ghosh, *J. Appl. Polym. Sci.* **2004**, *92*, 102–108.
[50] H. Kaplan Can, G. Karakus, N. Tuzcu, *Polym. Bull.* **2014**, *71*, 2903–2921.
[51] S. Wang, M. Wang, Y. Lei, L. Zhang, *J. Mater. Sci. Lett.* **1999**, *18*, 2009–2012.
[52] M. Coskun, P. Seven, *React. Funct. Polym.* **2011**, *71*, 395–401.
[53] G. Karakus, Z. Akin Polat, A. F. Yenidunya, H. B. Zengin, C. B. Karakus, *Polym. Int.* **2013**, *62*, 492–500.
[54] B. C. Smith, *Spectroscopy* **2015**, *30(1)*, 16–23.
[55] B. C. Smith, *Spectroscopy* **2015**, *30(4)*, 18–23.
[56] G. R. Saad, R. E. Morsi, S. Z. Mohammady, M. Z. Elsabee, *J. Polym. Res.* **2008**, *15*, 115–123.
[57] H. Patel, D. A. Raval, D. Madamwar, S. R. Patel, *Angew. Makromol. Chem.* **1998**, *263*, 25–30.
[58] J. John, M. K. Dalal, D. R. Patel, R. N. Ram, *JMS Pure. Appl. Chem.* **1997**, *A34*, 489–501.
[59] R. A. Tripp, R. A. Dluhy, Y. Zhao, *Nanotoday (Review)* **2008**, *3*, 31–37.
[60] H. Kaplan Can, A. L. Dogan, Z. M. O. Rzaev, A. H. Uner, A. Güner, *J. Appl. Polym. Sci.* **2005**, *96*, 2352–2359.
[61] H. Maeda, M. Ueda, T. Morinaga, T. Matsumoto, *J. Med. Chem.* **1985**, *28*, 455–461.
[62] M. A. Abbas, S. Hameed, J. Kressler, *Asian J. Chem.* **2013**, *25*, 509–511.
[63] F. Mustata, I. Bicu, *J. Optoelectron. Adv. Mater.* **2006**, *M. 8*, 871–875.
[64] O. Atıcı-Galioglu, A. Akar, R. Rahimian, *Turk. J. Chem.* **2001**, *25*, 259–266.
[65] F. Zafar, E. Sharmin, S. M. Ashraf, S. Ahmad, *J. Appl. Polym. Sci.* **2004**, *92*, 2538–2544.
[66] C. Z. Sun, C. T. Lu, Y. Z. Zhao, P. Guo, J. L. Tian, L. Zhang, X. K. Li, H. F. Lv, D. D. Dai, X. Li, *J. Nanomed. Nanotechnol.* **2011**, *2*, 2–6.
[67] L. F. Yaacoub, M. A. Aljuhani, A. Jedidi, M. S. Al-Harbi, W. Al Maksoud, W. Wackerow, E. Abou-Hamad, J. D. A. Pelletier, M. E. Eter, L. Cavallo, J. M. Basset, *Organometallics.* **2020**, *39*, 2438–2445.
[68] C. J. Cox, K. Dutta, E. T. Petri, W. C. Hwang, Y. Lin, S. M. Pascal, R. Basavappa, *FEBS Lett.* **2002**, *527*, 303–8.
[69] C. Kalalian, B. Samir, E. Roth, A. Chakir, *Chem. Phys. Lett.* **2019**, *718*, 22–26.
[70] N. M. Bikales, *Characterization of Polymers*, Wiley-Interscience, New York, **1971**, p. 264.
[71] A. Mishra, R. Dheepika, P. A. Parvathy, P. M. Imran, N. S. P. Bhuvanesh, S. Nagarajan, *Sci. Rep.* **2021**, *11*, 19324.
[72] E. Eshelman, M. G. Daly, G. Slater, E. Cloutis, *Planet. Space Sci.* **2017**, *25*, 1–10.
[73] D. D. Bozdoğan, G. Kibarer, Z. M. O. Rzayev, *Polym. Bull.* **2013**, *70*, 3185–3200.
[74] D.–X. Li, Y.-L. You, R.-F. Li, X. Deng, *J. Reinf. Plast. Compos.* **2013**, *32*, 1807–1820.
[75] M. Thilak, Q. Haiou, V. H. Desiree, M. A. Siyam, P. Angel, I. Taylor. *Nanomaterials for Food Applications, In Micro and Nano Technologies*, **2019**, pp 313–353. "Characterization of Nanomaterials: Tools and Challenges": A. L. Rubio, M. J. F. Rovira, M. M Sanz, L. G. Gómez-Mascaraque, Elsevier.
[76] A. Shrivastava, *Introduction to Plastics Engineering, Plastics Design Library*, William Andrew, PA, **2018**, p. 17.
[77] V. Kumar, A. Rana, C. L. Meena, N. Sharma, Y. Kumar, D. Mahajan, *Synthesis* **2018**, *50*, 3902–3910.
[78] S. Kanth, A. Nagaraja, Y. M. Puttaiahgowda, *J. Mater. Sci.* **2021**, *56*, 7265–7285.
[79] F. Liu, J. Hu, G. Liu, S. Lin, Y. Tu, C. Hou, H. Zou, Y. Yang, Y. Wu, Y. Mo, *Polym. Chem.* **2014**, *5*, 1381–1392.
[80] M. Haktaniyan, M. Bradley, *Chem. Soc. Rev.* **2022**, *51*, 8584–8611.
[81] M. D. Polêto, V. H. Rusu, B. I. Grisci, M. Dorn, R. D. Lins, H. Verli, *Front. Pharmacol.* **2018**, *9*, 395.
[82] M. Aldeghi, S. Malhotra, D. L. Selwood, A. W. Chan, *Chem. Biol. Drug Des.* **2014**, *83*, 450–61.

Manuscript received: May 11, 2023